Research papers

Heightened hurricane activity on the Little Bahama Bank from 1350 to 1650 AD

Peter J. van Hengstum [a,*], Jeffrey P. Donnelly [a], Michael R. Toomey [b], Nancy A. Albury [c], Philip Lane [a], Brian Kakuk [d]

[a] Department of Geology and Geophysics, Woods Hole Oceanographic Institution, Woods Hole, Massachusetts 02543, USA
[b] Massachusetts Institute of Technology/Woods Hole Oceanographic Institution Joint Program in Oceanography, Woods Hole, Massachusetts 02543, USA
[c] Antiquities, Monuments, and Museums Corporation, National Museum of The Bahamas, P.O. Box EE-15082, Nassau, The Bahamas
[d] Bahamas Caves Research Foundation, P.O. Box AB20755, Marsh Harbour, Abaco, The Bahamas

ARTICLE INFO

ABSTRACT

Deciphering how the climate system has controlled North Atlantic tropical cyclone activity through the Holocene will require a larger observational network of prehistoric hurricane activity. Problematically, the tropical North Atlantic is dominated by carbonate landscapes that typically preserve poorer quality coastal sediment records in comparison to their temperate-region counterparts (e.g., sedimentation continuity and rate). Coastal karst basins (CKBs), such as sinkholes, blueholes, and underwater caves, are widely distributed on carbonate platforms and contain overlooked sedimentary records. Here we present a millennium of hurricane deposits on the Little Bahama Bank archived in a 165 cm core that was extracted from 69 m below sea level in a bluehole on Great Abaco Island, The Bahamas. The coarse-grained overwash deposits associated with both hurricanes Jeanne (2004) and Floyd (1999) were identified using radioisotopes (^{137}Cs, ^{14}C, ^{210}Pb), and indicate that the bluehole is sensitive to hurricane-induced sedimentation. Over the last millennium, the Little Bahama Bank experienced heightened hurricane activity from 1350 to 1650 AD. The simplest explanation for this active interval is that favorable climate conditions (El Niño, West African Monsoon, and sea surface temperatures) encouraged North Atlantic hurricane activity at that time. However, asynchronous hurricane activity at similar latitudes in the North Atlantic and Gulf of Mexico suggest that regional oceanography has modulated or amplified regional hurricane activity over the last millennium.

1. Introduction

Any possible increase in North Atlantic hurricane frequency or intensity is quite ominous because tropical cyclones are a frequent source of coastal destruction and loss of human life (Goldberg et al., 2001; Elsner et al., 2008). According to recent predictions, average global tropical cyclone intensity may increase from 2% to 11% by 2100 (Knutson et al., 2010). However, regional ocean-atmospheric effects in specific oceanic basins will likely further influence tropical cyclone variability in response to future changes in climate (Maloney and Hartmann, 2002; Webster et al., 2005; Emanuel et al., 2008). Perhaps the best way to contextualize these forecasts in our currently warming climate is to understand how tropical cyclone climatology evolved by extending the short instrumental record with proxy-based tropical cyclone reconstructions.

Overwash deposits have emerged as the main technique for reconstructing prehistoric tropical cyclone events. Mckee and Blumenstock were likely the first to recognize the potential for reconstructing tropical cyclone events using their overwash deposits (Blumenstock, 1958; McKee, 1959; Blumenstock et al., 1961). Typoon Opelia struck Jaluit Atoll of the Marshall Islands on 7 January 1958 and deposited laterally-extensive gravel sheets (McKee, 1959; Blumenstock et al., 1961), leading Mckee (1959) to hypothesize that prehistoric overwash deposits would provide proxy evidence for tropical cyclones. Later, Emery (1969) documented and dated sand layers in the sediments from Oyster Pond, a coastal kettle basin on Cape Cod (Massachusetts), and inferred that they were overwash deposits from prehistoric hurricane strikes. Hurricane overwash deposits are now documented in lakes (Liu and Fearn, 1993, 2000), coastal wetlands (Donnelly et al., 2001b; McCloskey and Keller, 2009; Boldt et al., 2010), and back-barrier lagoons (Davis et al., 1989; Donnelly and Woodruff, 2007; Malaize et al., 2011; Park, 2012).

To explain the pattern of hurricane-related overwash deposits in a back-barrier lagoon, Donnelly and Woodruff (2007) posited

* Corresponding author. Tel.: +1 508 289 3985.
E-mail address: vanhengstum@whoi.edu (P.J. van Hengstum).

that intense hurricane events were inhibited by El Niño-like conditions and encouraged by the African Easterly Jet over the last 5.0 ka, similar to the modern climate system (Landsea, 1993; Goldenberg and Shapiro, 1996). However, modeled tropical cyclone climatologies forced to a constant El Niño state were unable to produce the reductions in activity observed in the paleo record (Woodruff et al., 2008). In contrast, others hypothesize that the North Atlantic Oscillation (NAO) or Intertropical Convergence Zone (ITCZ) may have forced latitudinal migration of an Atlantic hurricane belt through the Holocene (Liu and Fearn, 2000; Scott et al., 2003; McCloskey and Keller, 2009); interpretations which are also based on the instrumental record (Elsner et al., 2001; Elsner, 2003). Only by increasing our spatial network of prehistoric hurricane observations in the tropical Atlantic region will we understand how the climate system controlled prehistoric hurricane activity in the North Atlantic Ocean.

Problematically, the tropical Atlantic region is dominated by carbonate terrain, which has fewer coastal wetlands and lagoons suitable for paleo hurricane research. Hurricane overwash deposits have been recovered from tropical wetlands that developed on antecedent carbonate platforms (McCloskey and Keller, 2009). However, the sedimentation rate and continuity, and thus the resolution of these archives are limited by the accommodation space provided by sea-level rise, which has been relatively modest (≤ 0.5 mm yr^{-1}) over the last several millennia in the Atlantic Ocean (Fairbanks, 1989). Therefore, we need to develop more sedimentary environments with higher deposition rates to increase the spatial network of tropical paleo hurricane observations. Coastal karst basins (CKBs), which are features such as sinkholes, blueholes, and underwater caves, provide an alternative on carbonate landscapes (van Hengstum et al., 2011). Continual dissolution and modification of carbonate terrain over Quaternary time-scales creates a variety of basin-like features in limestone bedrock (Smart et al., 1988, 2006; Mylroie et al., 1995a, 1995b). In a recent study by Lane et al. (2011), a decadally-resolved and 4.5 ka record of hurricane activity in the Gulf of Mexico was preserved in a subaerial sinkhole (Apalachee Bay, Florida). In a submerged example, annually-laminated sediments containing hurricane-induced overwash deposits were described by Gischler et al. (2008) from a bluehole in Belize. These results indicate that sinkholes and blueholes may be an important, and largely overlooked, resource of paleo tropical cyclone deposits.

The purpose of this study is to examine sedimentation in a submerged Bahamian bluehole to (i) evaluate the suitability of submerged blueholes to paleo hurricane research, and (ii) provide evidence for prehistoric hurricane activity in the northwestern Caribbean region.

2. Regional setting

The archipelago of The Bahamas comprises multiple carbonate islands and shallow banks in the western North Atlantic Ocean, whose upper lithology is characterized by at least 10 km of highly-karstified shallow water carbonates (Mylroie et al., 1995b; Carew and Mylroie, 1997). The Little Bahama Bank is located in the northwestern region of the Bahamas and bordered by the North Atlantic Ocean and the Florida Straits (Fig. 1A). Two primary island groups are located on the Little Bahama Bank: The Abacos and Grand Bahama Islands (Fig. 1B). Thatchpoint Bluehole (TPBH) is a submerged bluehole on the western shallow shelf of Great Abaco Island (Fig. 1C), likely originating from both limestone dissolution and collapse events over the late Pleistocene (Mylroie et al., 1995a). Local SCUBA divers provide eyewitness evidence that a layer of hydrogen sulfide exists above the sediment–water interface in Thatchpoint Bluehole. This indicates that the sediment water interface is severely oxygen-depleted, caused by either flooding in by anoxic saline groundwater circulating through the carbonate platform, or localized oxygen depletion from the lack of circulation with the coastal ocean (Schwabe and Herbert, 2004; Steadman et al., 2007).

Hurricanes regularly strike The Bahamas because they are positioned along a major hurricane trackway of storms originating in both the Caribbean and Atlantic basins that then often translate north-westwards (Reading, 1990). Since 1850 AD, 10 tropical storms, 12 total hurricanes (category 1–5 on the Saffir–Simpson Hurricane Scale, this scale used hereafter) and 9 intense hurricanes (category 3–5) have passed within a 50 km radius of Thatchpoint Bluehole (http://csc.noaa.gov/hurricanes/#). The three most recent intense hurricane strikes on Abaco Island were Hurricanes Irene in 2011, Jeanne in 2004 and Floyd in 1999, each striking Great Abaco Island with category 3 intensity. Throughout the last century, the 1930s and 1940s saw a rapid increase in hurricane strikes to the Little Bahama Bank, but the number of hurricanes peaked in the 1940s and 1950s (Reading, 1990), similarly to the rest of the North Atlantic region (Goldenberg et al., 2001). On 17 September 1947 a category 5 hurricane passed about 50 km north of TPBH. A category 5 hurricane and category 4 hurricane passed directly over TPBH on 6 September 1932 and 6 October 1933, respectively. Three intense hurricanes passed near TPBH in the late 19th century. On September 6, 1896 a category 3 hurricane passed about 50 km east of the study site. A weak category 3 hurricane passed about 25 km north of TPBH on 22 August 1887 and a minimal category 4 storm passed about 45 km west of the site on 2 October 1866. According to newspaper records from the Bahamian capitol in Nassau, the 1830s was an especially active interval for increased gale force winds
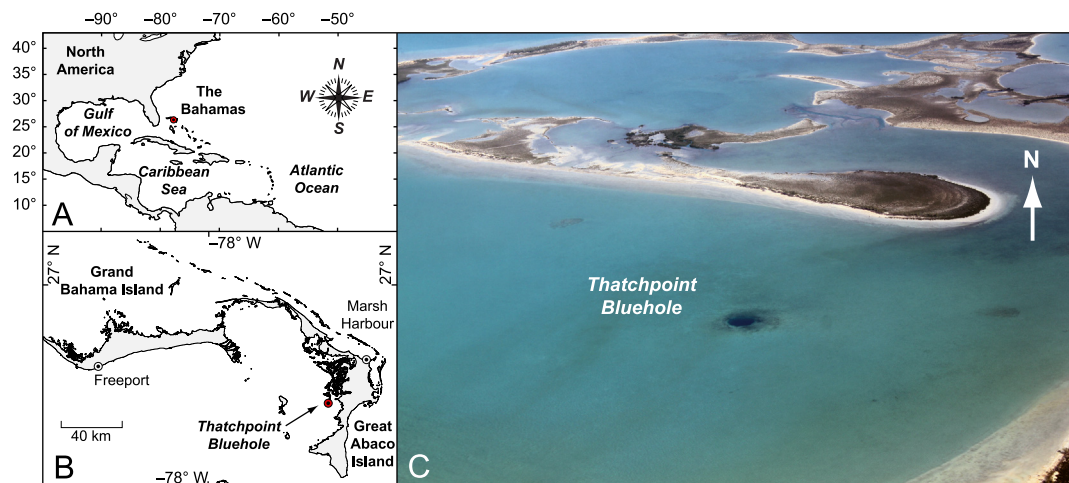
Fig. 1. Thatchpoint Bluehole (TPBH) is positioned in the northwestern Caribbean region (A) on the Little Bahama Bank between Grand Bahama and Abaco Islands (B). An oblique aerial photograph of TPBH (45 m diameter) identifying its position on the shallow shelf surrounded by sediment banks that are colonized by mangroves (C).

(Chenoweth, 1998). These instrumental and historical data are important for calibrating records of prehistoric storm activity from the Abaco Islands, The Bahamas.

3. Methods

In May 2011 AD, a 165 cm sediment push core (TPBH-C1) was collected on scuba from 69.2 ± 0.3 m below sea level (mbsl) in Thatchpoint Bluehole (26° 19.408′ N, 77° 17.590′ W). The core was collected before Hurricane Irene (category 3) hit Abaco Island in August 2011 AD. Back in the laboratory, the core was sectioned

lengthwise, X-radiographed, and sub-sampled at 5-mm intervals for sedimentological analysis. Grain size was continuously measured downcore on bulk sediment samples in a Beckman–Coulter LS13320 laser particle size analyzer, which measures particles with diameters ranging from 0.04 to 2000 μm with a precision of < 2 μm. Resultant particle size distributions (PSDs) were then plotted as a color surface plot, with no interpolation algorithm, to comprehensively visualize the sediment texture.

Loss on ignition (LOI) and sieving was performed on 5-mm intervals downcore to determine weight-percent (wt%) of organic matter content, coarse silt content (32–63 μm sized particles), and sand content (> 63 μm sized particles). First, sediment samples

Table 1

Radiocarbon results from articulated *Barbatia domingenesis* shells. All possible 1σ and 2σ age calibrations and their probabilities are provided, but only the highest probability 1σ calibration result was incorporated into the age model. AMS: traditional accelerator mass spectrometer method, CFAMS: continuous flow accelerator mass spectrometer method developed at Woods Hole Oceanographic Institution, no accession numbers or stable carbon isotopic ratios are available for these dates (McIntyre et al., 2011; Roberts et al., 2013).

Index no.	Lab number	Method	Core interval	Conventional ^{14}C age	Fraction modern (F^{14}C)	δ^{13}C (‰)	1σ Calibrated years AD (probability)	2σ Calibrated years AD (probability)	Highest probability 1σ date used in age model
1		CFAMS	2.5–3 cm		1.1234 ± 0.0162		1957.77–1958.00 (0.045) 1991.18–1991.21 (0.004) 1992.02–1992.38 (0.050) **1992.75–1996.07 (0.786)** 1996.40–1996.96 (0.113)	1957.58–1958.18 (0.065) **1990.84–1997.5 (0.935)**	**Oct 1992–Jan 1996**
2		CFAMS	31.5–32 cm		1.1301 ± 0.0168		1957.84–1958.06 (0.043) 1991.04–1991.49 (0.092) **1991.69 1995.77 (0.865)**	1957.64–1958.26 (0.64) 1989.91–1989.99 (0.004) **1990.22–1997.5 (0.931)**	**Sept 1991–Oct 1995**
3		CFAMS	37.5–38 cm		1.1563 ± 0.0132		1958.04–1958.35 (0.074) 1987.93–1987.96 (0.006) **1988.82–1991.98 (0.843)** 1992.42–1992.88 (0.075)	1957.84–1958.60 (0.084) 1986.94–1987.33 (0.017) **1987.78–1993.81 (0.899)** 1994.20–1994.20 (0.0002)	**Oct 1988 Dec 1991**
4		CFAMS	50.5–51 cm		1.2971 ± 0.0147		1961.89–1962.23 (0.195) 1977.94–1977.99 (0.017) **1978.78–1979.98 (0.740)** 1980.47–1980.59 (0.046)	1961.77–1962.36 (0.168) 1976.93–1976.98 (0.002) **1977.79–1980.88 (0.807)** 1981.08–1981.15 (0.003) 1981.39–1981.95 (0.196)	**Oct 1978–Dec 1979**
5		CFAMS	59.5–60 cm		1.2341 ± 0.0142		**1959.61–1961.67 (0.521)** 1982.12–1984.08 (0.478)	**1958.75–1961.79 (0.472)** 1980.19–1980.20 (0.0004) 1980.89–1985.03 (0.514)[a] 1985.41–1985.69 (0.013)	**Aug 1959–Sept 1961**
6	OS-94358	AMS	65.5–66 cm	70 ± 25	0.9912 ± 0.0032	1.48	**1880–1915 (0.581)** 1819–1833 (0.167) 1706–1720 (0.194) 1700–1702 (0.026)	**1866–1919 (0.488)** 1812–1863 (0.246) 1694–1727 (0.247)	**1880–1915**
7		CFAMS	73.5–74 cm		0.97405 ± 0.0143		1649–1694 (0.249) **1726–1813 (0.480)** 1837–1842.19 (0.018) 1852–1867 (0.065) 1874–1875 (0.005) 1917–1951 (0.179)	1649.99–1713.65 (0.232) **1715.47–1891.16 (0.610)** 1908.01–1951.86 (0.158)	**1726–1813**
8[a]	OS-94562	AMS	94–95 cm	550 ± 25	0.9337 ± 0.0029	1.83	1328–1341 (0.292) **1395–1419 (0.708)**	1317–1354 (0.380) **1317–1354 (0.620)**	**1395–1419**
9A[b]		CFAMS	123.5–124 cm	428 ± 116	0.9481 ± 0.0137		**1409–1529 (0.615)** 1544–1548 (0.014) 1550–1634 (0.369)		
9B	OS-90998	AMS	123.5–124 cm	605 ± 30	0.9271 ± 0.0035	1.2	**1304–1330 (0.401)** 1338–1364 (0.415) 1384–1397 (0.183)	**1297–1405 (1)**	**1304–1330**
10		CFAMS	158.5–159 cm	962 ± 116	0.8871 ± 0.0129		**987–1208 (1)**	**860–1277 (0.987)** 820–842 (0.011) 783–787 (0.002)	**987–1208**

[a] This sample was excluded from age model based on stratigraphic arguments.
[b] This sample was excluded from age model because the alternate valve measured by standard AMS techniques provided smaller analytical uncertainty (9B).

were dried overnight at 105 °C, weighed, combusted at 550 °C for 4.5 h, and re-weighed to determine the relative contribution of organic matter to the sedimentary dry mass (Heiri et al., 2001). Replicate samples had a typical precision of less than ± 2%, which is typical for the method. After combustion, the remaining ash and inorganic sediment was wet sieved over > 32 μm and > 63 μm meshes to retain the coarse silt and sand fractions, dried overnight at 105 °C, and reweighed to calculate their weight percent relative to the original sample. These coarser grained sediments were then stereo-microscopically examined to determine their petrographic character.

Radiocarbon dating of 10 marine bivalves (*Barbatia domingensis*) provide the primary age control for the core. Planktonic foraminifera were not present, and benthic foraminifera would likely be unreliable chronometers because of taphonomic issues (discussed below). In contrast, *B. domingensis* is short-lived (< 5 yr) and sessile bivalve that is known to live in underwater caves and in reef cavities by attaching itself to hard substrates in oxygenated waters (Logan et al., 1984; Kobluk and Lysenko, 1986; van Hengstum et al., 2011). The *B. domingensis* recovered from TPBH were most likely attached to the carbonate wall of the bluehole in the oxygenated water column, and sank to the blue-hole bottom upon death to become part of the sediment record. Thus, radiocarbon dating *B. domingensis* can avoid problems associated with pore water effects on infaunal taxa, or taphonomic effects imparted to other transported coastal bivalves. Only articulated bivalves were measured to help reduce taphonomic problems associated post-mortem transport of the animal. Three samples were aged by traditional AMS measurements, while eight samples were dated using the Continuous Flow AMS (CFAMS) method at the National Ocean Sciences AMS facility at Woods Hole Oceanographic Institution (McIntyre et al., 2011; Roberts et al., 2013). As a simple test of reproducibility, each valve from one single articulated *B. domingensis* (123.5–124 cm) was dated by each method: 9A was dated by CFAMS, and 9B was dated by traditional AMS (Table 1). The results from both techniques are within 2σ uncertainty, and demonstrate the applicability of the CFAMS technique. Conventional radiocarbon ages with a fraction modern value ($F^{14}C$) that was less than 1.0000, thus indicating a sample that was alive pre-1950 AD, was calibrated with IntCAL09 (Reimer et al., 2009) because no reservoir effect was detected at the site (see Section 4.2 for details). However, radiocarbon dates with a fraction modern value ($F^{14}C$) exceeding 1.0000 were calibrated with CALIbomb (Reimer et al., 2004), using the compiled Northern Hemisphere Zone 2 dataset (Hua and Barbetti, 2004), because these samples were alive post-1950 AD.

To verify the radiocarbon chronology, radioisotopes were used to further establish the chronology of the core during the historic period. ^{137}Cs is a man-made radionuclide that can identify the initiation (~1954 AD) and moratorium (~1963 AD) on nuclear weapons testing based on ^{137}Cs concentration in bulk sediment (Pennington et al., 1973). Furthermore, ^{210}Pb is helpful for dating historic sediments because supported ^{210}Pb activity in the sediment is constant, whereas the unsupported ^{210}Pb activity from atmospheric fallout follows exponential decay over the last ~150 years (Robbins and Edgington, 1975). ^{137}Cs and ^{210}Pb activity was measured on desiccated and powdered bulk sediment samples from 1-cm intervals throughout the core in a Canberra GL2020RS low-energy Germanium gamma well detector.

4. Results

4.1. Sedimentary characteristics

Upon first visual inspection, laminated carbonate sediments with distinct sand layers characterized the stratigraphy (Fig. 2).
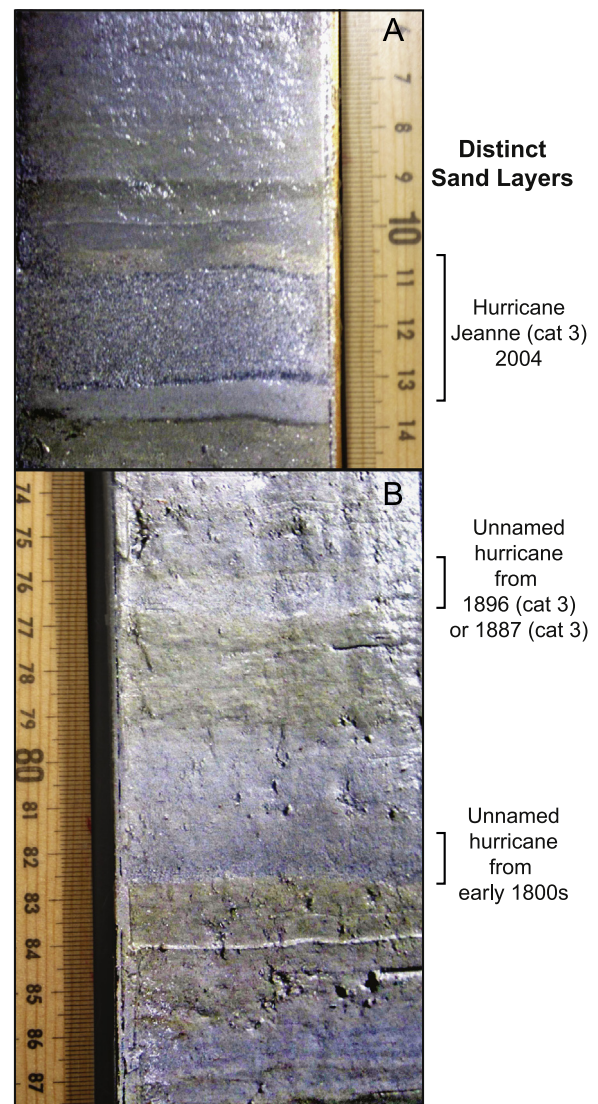

Fig. 2. Photographs depicting examples of the distinct sand layers observed in the core. (A) Sand overwash deposit at 11–12 cm coinciding with Hurricane Jeanne in 2004; (B) analogous sand overwash deposits at 76–76.5 cm and 82–82.5 cm.

The core contained a mean 8.8% bulk organic matter, ranging between 4.3% and 12.8% (Appendix 1). However, none of this organic matter was identifiable plant fragments (e.g., sea grasses, algae); just fine-grained particles in the sedimentary matrix. Further analysis by x-radiography revealed the laminations as distinct density alternations downcore as well as the textural changes (Fig. 3). These results indicate that negligible post-depositional reworking has occurred through either bioturbation or wave action. *B. domingensis* shells and serpulid worm tubes were the primary macroinvertebrate remains in the sediment; and other mollusks were almost never encountered. The benthic dysoxia in the bluehole can easily account for promoting the laminated stratigraphy, the absence of benthic gastropods that typify tropical marine environments, and only sessile marine invertebrates dropping off the vertical bluehole walls.

Eleven visually distinct sand layers were juxtaposed against the laminated fine-grained carbonate mud (e.g., 10–12 cm; 23–25 cm). Based on laser particle size analysis, the mean grain size throughout the core typically ranged between 15 and 25 μm (Fig. 3), or fine to medium silt. The distinct sand layers can be readily observed in the color surface plots of the particle size distributions with a marked shift to a higher volume of coarser sediment (Fig. 3).
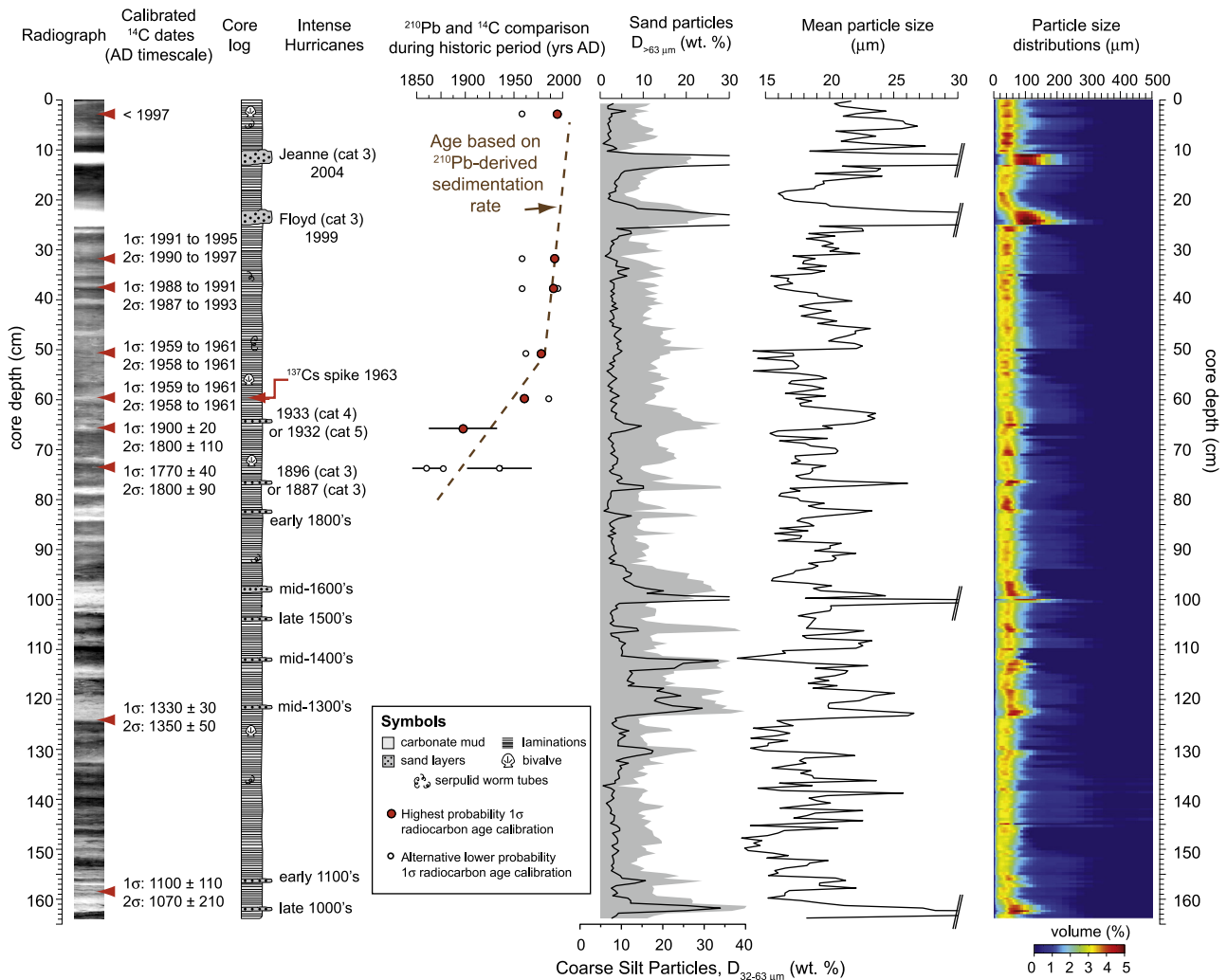
Fig. 3. The sedimentary and textural characteristics in TPBH-C1. The radiocarbon ranges listed are the highest probability 1σ range on the calibrated age, and the uncertainty in the age determinations increases below 65 cm. See Fig. 4 for detailed geochemical profiles. The online version of this figure appears with color.

However, there are additional intervals downcore where the volume of coarse sediment increases with a more broad particle size distribution (e.g., 110 cm), prompting further examination of just the coarse sediment fraction (> 32 and ≥ 63 μm).

In contrast to the mean grain size metric and PSDs, which examined total sediment distributions including organic matter, the sieving procedure specifically reveals downcore variation in the coarse silt (32–63 μm) and sand (> 63 μm) fractions, independent of organic matter. All 11 visually distinct sand layers correspond to peaks in the coarse sand to > 8% sand, and the coarse silt to > 22%. These horizons also were denser (lighter hued) horizons in the x-radiograph. Interestingly, the peak in sand fraction at 135 cm was not associated with a visually distinctive sand layer, meaning that visual inspection techniques cannot be solely relied upon to evidence coarse-grained textural changes (i.e., sand layers). Not all dense horizons indicated in the x-radiograph exclusively correspond to an increase in sand deposition. For example, at 37 cm there is denser horizon that corresponds to increased deposition of finer grained sediments (mean grain size shifts to ~15 μm, Fig. 2), likely with tighter particle packing in the fabric. This indicates that although the x-radiograph is faithfully indicating down-core density changes, not all density alternations directly relate to an increase in sand deposition.

The coarse silt (> 32 μm) and sand (> 63 μm) fractions are dominated by benthic foraminifera, especially miliolids (e.g., Quinque-loculina, Triloculina), and occasional shells from B. domingensis and

serpulids worm tubes. Considering that (i) the benthos in the bluehole is oxygen deprived, (ii) miliolid foraminifera are intolerant to dysoxia, and (iii) the shallow Bahamian shelf is dominated by these shallow water miliolids, the simplest explanation is that these coarse sediments are being transported into the bluehole from the surrounding shallow shelf. Considering the abundance of planktonic foraminifera in the tropical Atlantic Ocean, the lack of planktonic foraminifera in the bluehole succession indicates the sediment is most likely derived from local sources (shallow shelf and coastal regions).

4.2. Chronology, age model and sedimentation rates

The radiocarbon dates are properly ordered and suggest continual deposition in the bluehole over the last millennium. The oldest radiocarbon date is from 158.5 to 159 cm and aged to 1100 ± 110 AD (Table 1). The youngest radiocarbon date is from the core top at 2.5–3 cm and aged from 1992 to 1996 AD. However, because the CALIbomb dataset curve that was used can only date samples younger than 1997 AD (dataset limit), this result is not unexpected and consistent with a very recent age for the core top. The radiocarbon results suggest a rapid increase in sedimentation between 50 and 70 cm core depth. The topmost 60 cm of core was deposited in ~50 years, whereas the bottom 1 m was deposited over the last millennia (discussed further below). The radioiso-topes were used to provide further insight into this apparent

change in sedimentation rate, and also confirm the absolute ages determined by the radiocarbon results.

Based on the radiocarbon dating, the 1950 AD chronohorizon should occur above 65 cm, when $F^{14}C$ exceeds 1.0000 (Fig. 4A) (Reimer et al., 2004). Two peaks in ^{137}Cs activity (> 4.5 Bq/g $\times 10^{-3}$), within analytical uncertainty, occur at 60 cm and 70 cm depth, thus confounding a simple interpretation of a 1963 AD chronohorizon (Fig. 4B). However, considering the fraction modern ($F^{14}C$) exceeds 1.0000 above 65 cm, the simplest explanation is that the ^{137}Cs peak at 60 cm is the 1963 AD chronohorizon related to the moratorium on nuclear weapons testing. Furthermore, the calibrated age of the radiocarbon sample at 59.75 cm is 1960 AD (Index Point 5, Table 1), which also corresponds with the ^{137}Cs results. The low ^{137}Cs activity deeper in the core is challenging to attribute to bioturbation given the laminated stratigraphy and benthic dysoxia previously discussed. A possible explanation may be that downward vertical mobilization of ^{137}Cs is occurring aided by pore fluid migration, which even if occurs, does not effect the stratigraphic position of the 1963 AD chronohorizon from ^{137}Cs (Robbins and Edgington, 1975). Importantly, the position of the ^{137}Cs peak does confirm the radiocarbon results.

The ^{210}Pb data independently confirm both the ^{137}Cs and ^{14}C data, including the change in sedimentation rate at 51 cm, which further indicates a cohesive stratigraphic record. Historical sediment profiles contain ^{210}Pb activity from two sources: long-term stabilized background supported ^{210}Pb activity in the sediment, and atmospherically-derived unsupported ^{210}Pb activity. The rise in ^{210}Pb activity in sediment profiles indicates a remaining contribution from unsupported ^{210}Pb activity, and coincides with the mid-nineteenth century (Robbins and Edgington, 1975). In the core from TPBH, the rise in ^{210}Pb activity occurs above 80 cm. When the average value of the supported ^{210}Pb activity ($n=6$, 160–80 cm depth) is subtracted from the total ^{210}Pb activity, and the anomalously low ^{210}Pb activity from event horizons is ignored (20–26 cm), a broad exponential increase in ^{210}Pb activity occurs upcore (Fig. 4C). By plotting the resultant unsupported ^{210}Pb activity on a log normal plot, two distinct linear trends emerge with an inflection point at 51.5 cm, which indicate that sedimentation rate increased above this point (Fig. 4D). These results also closely accord and verify with the increase in sedimentation rate from 50 to 70 cm that is evidenced by the radiocarbon dates (Fig. 3).

Another implication of these radioisotopic results is that no marine reservoir effect is influencing the radiocarbon signature in the *B.*

domingensis shells. If a reservoir effect did influence the radiocarbon composition of the shell, one would expect the bivalves to have a considerably lower fraction modern value ($F^{14}C$), which in turn would be indicative of an older age. However, the ^{210}Pb rise at ~70 cm indicates a mid-nineteenth century age (~1850 AD), and the IntCAL09 calibrated age of radiocarbon date at 73.5 cm is just slightly older with a 1σ range of 1726–1813 AD (Index Point 7, Table 2). A similar relation can be established between the radiocarbon age from the bivalve at 59 cm calibrated with CALIbomb and the ^{137}Cs peak at 60 cm, within analytical uncertainties. Therefore, the marine bicarbonate pool (HCO_3^-) at TPBH is in equilibrium with the atmospheric pCO_2 pool, likely from routine wave action and oceanic mixing on the shallow shelf, and precluding a marine reservoir effect from impacting the bivalves. Thus, the radiocarbon dates from the marine bivalves were calibrated with IntCAL09 (Reimer et al., 2009) and CALIbomb (Reimer et al., 2004).

An age model and sedimentation rates were calculated by linear interpolation between prehistoric radiocarbon tie-points prior to 1869 AD (Table 1), and thereafter the linear sedimentation rates derived from the unsupported ^{210}Pb profile (Fig. 5). This model ignores event-driven sedimentation, but this is a reasonable approach given the age uncertainties. To avoid circular reasoning, the ^{137}Cs data (1963 AD tie-point) was not included in the age model, which is arguably redundant because it conforms to the unsupported ^{210}Pb profile. Radiocarbon Index Point 9A was excluded from the model as Index Point 9B provided smaller analytical uncertainty. Index Point 8 was also excluded from the age model because likely unreasonable sedimentation patterns must be invoked to explain its inclusion into the chronology. For example, one would have to argue that only 15 cm of sediment accumulated in the bluehole in ~450 years, a scenario that is highly unlikely given: (i) the historic sedimentation patterns, and (ii) neither the wave climate nor adjacent sedimentary budgets have shifted in the last millennium to explain any rapid decrease in—then resumption of—sedimentary influx into Thatchpoint Bluehole. One could posit that the locale of sedimentation perhaps shifted through time at the base of the bluehole, resulting in an apparent change in sedimentation rate, because not all 'sand horizons' are stratigraphically continuous in the much larger (320 m diameter) Great Blue Hole, in Belize (Gischler et al., 2008). However, this seems improbable given the (i) quite narrow diameter of Thatchpoint Bluehole (45 m), and (ii) the lack of a mechanism ceasing sedimentation in the central region at the base of
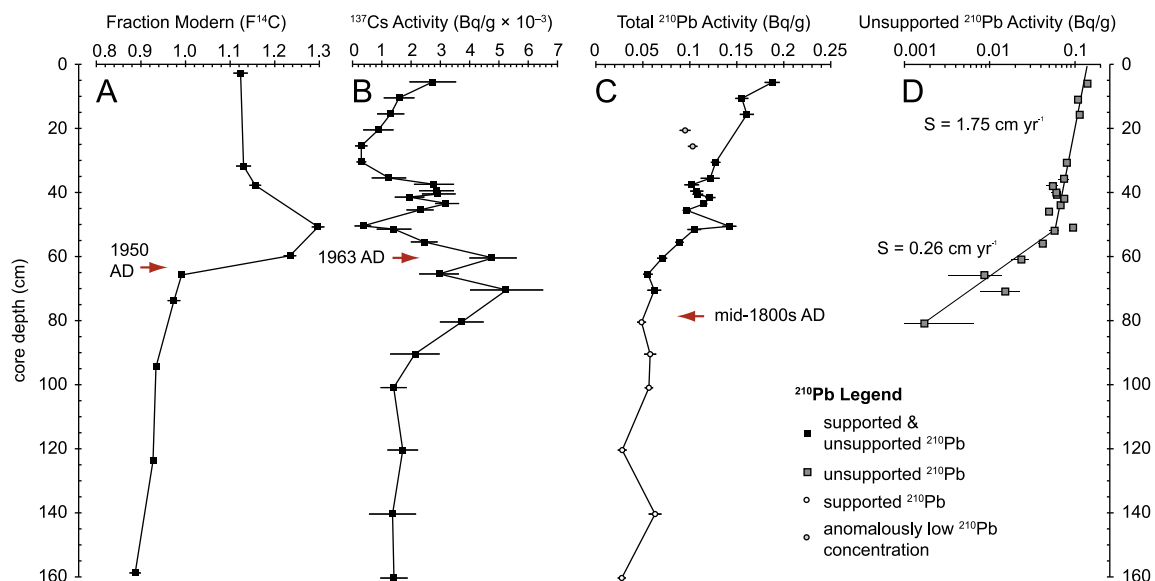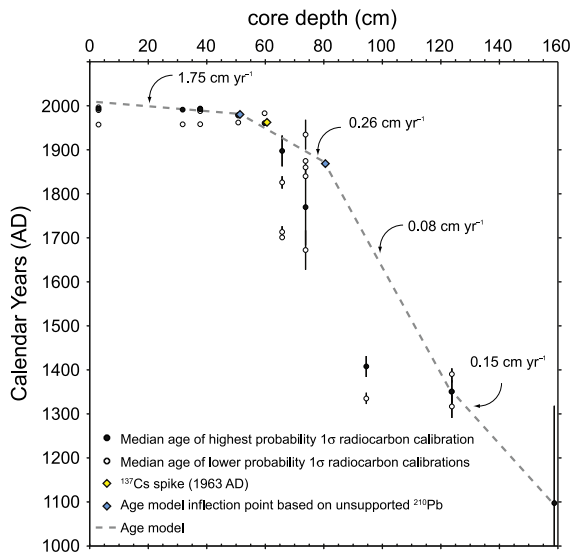

Fig. 4. The position of the ^{14}C and ^{137}Cs chronohorizons in the core, based on bivalves and bulk sediment, respectively. The total and unsupported ^{210}Pb activity also supports the chronology of the nuclear bomb radioisotopes, note the change in sedimentation rate at 51 cm depth. S: sedimentation rate.

Fig. 5. Complete geochronologic data and sedimentation rates for TPBH-C1 and note the coherency between all three geochronometers during the historic period. All possible 1σ calibration results from radiocarbon dates with their uncertainties are shown, and the text explains the stratigraphic arguments for omitting the radiocarbon date at 94.5 cm from the final age model. The age model is based upon the ^{210}Pb results from 0 to 80 cm depth, and the radiocarbon dates from 80 cm to 156 cm (gray dashed line).

the bluehole, which behaves as a giant settling column. In contrast, taphonomic principles provide the simple reason that the *B. dom-ingensis* individual for Index Point 8 (Table 1) simply did not become part of the sediment record upon death of the organism, and thus is excluded from the age model.

Sedimentation rates are not constant throughout but gradually increase upcore (Fig. 5). The sedimentation rate from approximately 1100 to 1300 AD is 0.15 cm yr^{-1}, which changed only modestly to 0.08 cm yr^{-1} from approximately 1300–1870 AD. Sedimentation rate then increases from 1870 to 1981 AD to 0.26 cm yr^{-1}, and thereafter to the present rate of 1.75 cm yr^{-1}. These sedimentation rates mean that individual storm events can potentially be represented in the stratigraphic record during the historic period, but the prehistoric period may biased toward undercounting of potential storm activity through prehistory because of lower sedimentary resolution.

5. Discussion

5.1. Basin sensitivity analysis

It is important to evaluate the suitability of a sedimentary basin for reconstructing paleo hurricane events. Ideal basins: (i) are sensitive to hurricane sedimentation, (ii) promote the long-term preservation and isolation of hurricane overwash deposits from subsequent re-working, (iii) have sufficient background sedimentation that is juxtaposed from hurricane sedimentation, and (iv) have a geometry or geomorphologic setting that prevents, or limits, the effects of sea-level change and landform dynamics from confounding the hurricane signal in the sedimentary record. Overall, sedimentation in TPBH has been continuous over the last millennium with excellent preservation, as evidenced by the laminated stratigraphy (Fig. 3). The benthic anoxia in TPBH minimizes bioturbation, and the sediment water interface at the bottom of the bluehole is far removed from post-depositional reworking by coastal currents or wave action. The stabilized morphology of the karst basin, namely the limestone bedrock, further minimizes the effect of sea level changing the sensitivity of

basin through time. This is in stark contrast to back barrier lagoons and salt marshes that are sensitive to barrier dynamics and where accretion rates are controlled by sea-level changes.

In general, neither the sedimentation rate nor carbonate mud deposition into TPBH are exclusively linked to storm activity. One would suspect that since bluehole sedimentation appears primarily allochthonous, then sedimentation rate may be positively correlated with storm activity. However, hurricane activity in the North Atlantic and The Bahamas increased from occurred from the mid-1920s through 1970 (Reading, 1990; Goldenberg et al., 2001), yet this interval does not correspond to any detectable change in sedimentation rate (Fig. 5). Furthermore, the sedimentation rate increased at approximately 1981 AD, which is actually the onset of a rather quiescent decade of hurricane activity in the North Atlantic (Goldenberg et al., 2001), so sedimentation rate in TPBH is not correlated to storm activity. Fine carbonate mud (mean particle sizes of 15 and 25 μm) is the primary sedimentary constituent (Fig. 2), which likely originates from local biological processes (algal precipitation, diagenesis of skeletal grains) or directly precipitates from seawater (Gischler and Zingeler, 2002). Therefore, other variables must be used to generate proxy evidence of hurricane events at TPBH, and the coarse silt and sand deposition is related to hurricane activity on the Little Bahama Bank.

Three distinctive sand layers developed during the instrumental period that are coeval with intense hurricanes passing within a 50 km radius of TPBH (Figs. 3 and 6A): (i) Hurricane Jeanne passed as a category 3 event in 2004 (overwash deposit at 11 cm),
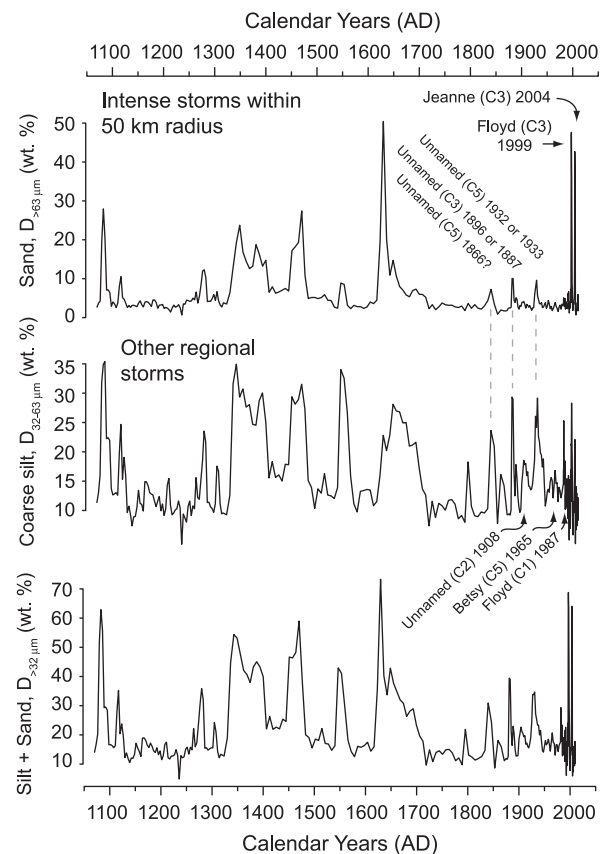
Fig. 6. Sand (A) and coarse silt (B) deposition into TPBH over the last millennium. Peaks in coarse-grained sediment are associated with known hurricane events striking within a 120 km radius of TPBH are noted. After a sensitivity analysis of TPBH during the historic period, the combined sand and silt data (C) provide the most faithful record of long-term hurricane activity, thus providing proxy evidence for active versus quiescent intervals of hurricane activity at TPBH over the last millennium.

(ii) Hurricane Floyd passed as a category 3 event in 1999 (overwash deposit at 22 cm), and (iii) and the sand layer at 64 cm likely records unnamed intense events in 1932 AD (cat. 5) and 1933 AD (cat. 4) that passed directly above TPBH (overwash deposit at 64 cm). Due to uncertainties in our age model, it remains challenging to accurately date the overwash deposit at 74 and 82 cm, but the horizon at 74 cm is very close to the age of known category 3 events in 1886 or 1887, and the deposit at 82 cm is perhaps the event the struck in the early 1800s. On 17 September 1947, a category 5 hurricane passed 50 km north of TPBH, but this storm did not leave a distinctive overwash deposit. Thus, the 1947 event suggests that a direct strike from an intense hurricane is required to generate distinctive visual sand layers in the stratigraphic record. Considering the TPBH succession documents all intense hurricane strikes in the instrumental period striking within a 50 km radius of the site, it is reasonable to assume that the six distinctive sand horizons deeper in the succession also document intense hurricane events striking TPBH. In total, the 11 classic hurricane overwash deposits are comparable to the hurricane overwash deposits in Great Blue Hole, Belize (Gischler et al., 2008), where distinct sand layers are juxtaposed with laminated and fine-grained carbonate mud.

The coarse silt sedimentation in TPBH during the historical period has also documented hurricane activity, and peaks in coarse silt can be correlated to either (i) local weak hurricane events, or (ii) more intense hurricane events traveling more distal to TPBH. However, the record of these events in the sediment record has a poorer fidelity than the coarse sand deposition (Fig. 6B). The increases in coarse silt sedimentation simultaneous with increased sand deposition are no doubt related to the same event, but there are several other increases in coarse silt deposition occurring independent of peaks in sand deposition. Many of these peaks in coarse silt can be associated to specific hurricane events in the instrumental record. The first example is the peak in coarse silt deposition to $>25\%$ at 49 cm, and although the age model assigns an age of 1983 to this datapoint, this is within age uncertainty of a different Hurricane Floyd that passed 46 km to the north of TPBH on 14 October 1987 AD as a strengthening tropical storm that achieved hurricane status south of Florida. Secondly, there is a peak in coarse silt at 55.75 cm to $>25\%$ that is aged to 1965 AD, which is the year Hurricane Betsy passed 86 km to the south of TPBH has a category 3 event. Lastly, there is a peak in coarse silt at 70.25 cm aged to 1908 AD, a year when a Unnamed category 2 hurricane event that passed less than 3 km away from TPBH (Fig. 6B). However, there were many other weaker storms that passed by TPBH during the historical period that are not recorded in the stratigraphy, indicating that coarse silt deposition is biased for undercounting hurricane events. This is not surprising, considering most sediment archives are biased in this manner. When considered collectively, however, these results indicate that the coarse silt deposition into TPBH can be used more cautiously as a proxy for weaker hurricanes passing nearby, or stronger hurricanes passing further away.

Taken collectively, both the sand and coarse silt sedimentation into TPBH provide proxy evidence for hurricane activity on Great Abaco Island (Fig. 6C). Over the last millennium, the hurricane reconstruction from TPBH (Fig. 6C) indicates distinct active versus quiescent intervals of hurricane activity. Intense hurricane events are more frequent from 1050 to 1150 AD, followed by an interval of quiescence until about 1350 AD. Sand and coarse silt deposition increase the most between roughly 1350 and 1650 AD (Fig. 6), suggesting that this interval coincides with the greatest relative increase in hurricane activity at TPBH. Intense hurricane events ($>$ category 3) appear to become infrequent from the early 1600s to the early 1800s, although weak local or distant strong storms (based silt deposition) appear persistent until 1700 AD. These results are consistent with the Spanish archives, which document fewer Atlantic hurricane events from 1600 to 1750 AD (García-Herrera et al., 2005). Increased hurricane activity again resumes in the late 1700s demarcated by an increase in sand deposition into the bluehole, results that are consistent with historical evidence (Reading, 1990). Despite the dating uncertainties, several main points emerge from the TPBH hurricane reconstruction: (1) historic intense hurricane events passing within 50 km radius of TPBH were faithfully recorded in the TPBH stratigraphic record by distinct sand deposition, (2) specific weak proximal hurricanes or intense distal hurricanes caused an increase in coarse silt sedimentation, and (3) there are distinct intervals of increased versus decreased coarse sedimentation through time (Fig. 6C), that after considering their calibration to the instrumental record, can be taken to represent active versus quiescent intervals of hurricane activity during the last millennium. Most obviously from the reconstruction, an interval of heightened hurricane activity occurred in the northern Bahamas from approximately 1350 to 1650 AD, however, further age control is necessary in order to better constrain the age of this interval.

5.2. Climate forcing of hurricane activity on the Little Bahama Bank

Our understanding of how the Late Holocene ocean–climate system has controlled hurricane genesis, maturation and their tracks to higher latitudes still remains poorly understood. This likely relates to the complex interactions of climate variables that are certainly working together to regulate long-term North Atlantic hurricane activity. However, one of the most important factors generating modern hurricanes in the Main Development Region (MDR) between $10°$ and $20°N$ in the North Atlantic is African Easterly Waves. Over 80% of intense hurricanes and 60% of named storms can be attributed to disturbances from the African Easterly Jet, which increases cyclonic vorticity in the MDR (Landsea, 1993; Goldenberg and Shapiro, 1996). Modern instrumental data provides a positive correlation between a well-developed African Easterly Jet, Atlantic hurricanes and tropical African precipitation (Bell and Chelliah, 2006), indicating that the behavior of the West African Monsoon may inform long-term patterns of extreme hurricane events (Donnelly and Woodruff, 2007). Reconstructions of precipitation in western Africa from Ghana and Cameroon suggest that an invigorated (dampened) African Easterly Jet contributed to increased (decreased) hurricane activity at TPBH over the last millennium (Fig. 7). The period of decreased hurricane activity from 1100 to 1350 AD corresponds to evidence for relative drought from Lake Ossa (Cameroon) and a dampened African Easterly Jet, and conversely, the active interval from 1350 to 1650 AD corresponds to an active African Easterly Jet (Nguetsop et al., 2004). This suggests that a poorly developed African Easterly Jet reduced potential cyclonic vorticity in the MDR from 1100 AD to 1350 AD, in turn hampering North Atlantic hurricane activity. However, a more recent higher-resolution reconstruction of precipitation from Lake Bosumtwi (Ghana) in the western Sahel suggests a more complex pattern of the West African Monsoon over the last millennium (Shanahan et al., 2009). Precipitation at Lake Bosumtwi increased from the 1100s to 1350 AD, coinciding with lower hurricane activity at TPBH. Precipitation then decreased to a minimum from 1350 AD to the late 1500s (Shanahan et al., 2009), thus suggesting that a dampened West African Monsoon coincided with the latter portion of the interval of heightened hurricane activity observed at TPBH. The lack of direct correlation between precipitation proxies in western Africa and the TPBH hurricane record hampers unequivocal understanding of how the West African Monsoon impacted hurricane activity in the North Atlantic from ~1500 to 1650 AD. However, if the higher-resolution record from Lake Bosumtwi (Ghana) is taken as more informative for potential cyclonic vorticity in the North Atlantic over the last millennium, then the onset of the active interval at from
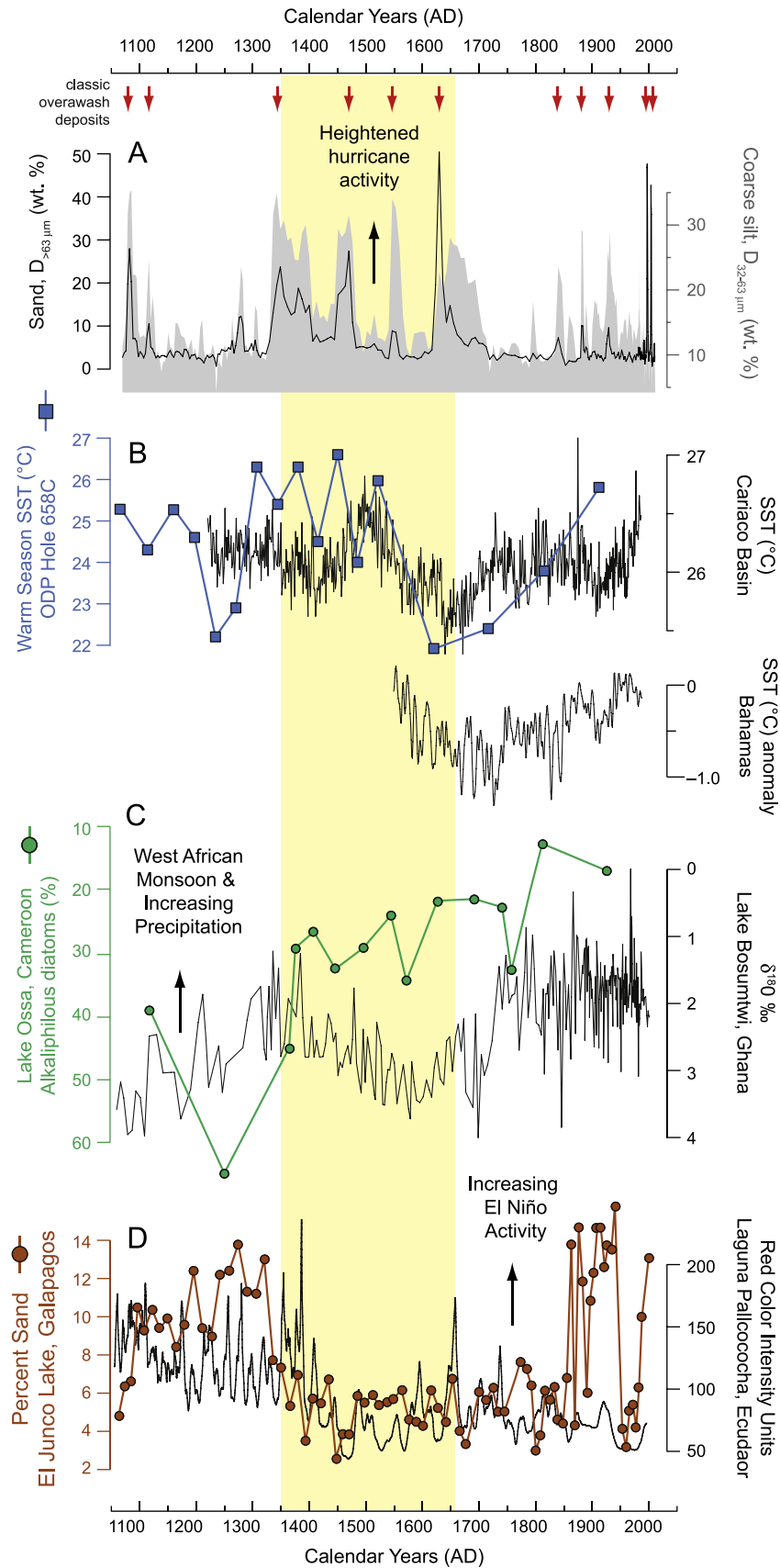
Fig. 7. Hurricane activity in the northern Bahamas compared to primary drivers of Atlantic hurricane activity. (A) Reconstruction of general hurricane activity over the last millennium on Great Abaco Island as recorded in TPBH, (B) sea surface temperature (SST) reconstructions from the Cariaco Basin (Black et al., 2007), ODP Hole 658C off the west coast of Africa in the Main Development Region (deMenocal et al., 2000), and SST anomaly recorded in Bahamian coral (Saenger et al., 2009); (C) long-term precipitation in western Africa from Ghana (Shanahan et al., 2009) and Cameroon (Nguetsop et al., 2004) can provide evidence for a changing West African Monsoon; and (D): proxy evidence for El Niño-like precipitation events in Ecuador (Moy et al., 2002) and the Galapagos (Conroy et al., 2008). The red arrows at the top of this figure refer to the location of coarse-grained sand layers that could be visually observed downcore, which are depicted in Fig. 2. The online version of this figure contains color.

1350 to 1650 AD is likely correlated to an invigoration of the African Easterly Jet, but the sustainment of this interval must be related to other climate forcings.

Sea surface temperature (SST) remains an important predictor for hurricane formation on an inter-annual basis because the oceans are the primary energy source for hurricanes (Shapiro and Goldenberg, 1998; Webster et al., 2005; Dailey et al., 2009). Warm SSTs also act to reduce mean vertical wind shear in the MDR, in turn increasing the likelihood for hurricane development (Shapiro and Goldenberg, 1998). No SST record is available from the MDR, but SSTs are available for both the eastern region of the Main Development Region (MDR) off the western coast of Africa (ODP Hole 685C) and on the western periphery of the MDR from the Cariaco Basin (Fig. 7). Both areas experienced warmer SSTs from the late 1200s to mid-1500s, directly coinciding with the onset of the active hurricane interval observed by TPBH. Similarly, periods of quiescent hurricane activity in the late 1200s coincide with cool SSTs at Hole 685C (deMenocal et al., 2000). However, the SST record from Hole 685C must be cautiously used for representing SSTs throughout the MDR because that site is a known upwelling region.

Near the end of the active interval from 1350 to 1650 AD, however, elevated SSTs are not coincident with the heightened hurricane activity observed at TPBH. For example, the early 1600s experienced markedly cooler temperatures at Hole 685C, the Cariaco Basin, and in the western Sargasso Sea (Keigwin, 1996; deMenocal et al., 2000; Black et al., 2007). More locally, a Bahamian coral-based SST reconstruction indicates that 1600–1750 AD was the coldest period of the last 500 years (Saenger et al., 2009), similar to the high-resolution reconstruction from the Cariaco Basin (Fig. 7). A similar anti-phase relation between hurricane activity and SSTs can be observed around 1900 AD (Fig. 7). As discussed by Michaels et al. (2006), however, cyclogenesis and SST is not a simple cause- and effect-relationship, because the thermal gradient between the sea surface and upper troposphere is the key factor.

Modern climatological analysis indicates that El Niño events suppress North Atlantic hurricane activity by increasing the vertical wind shear in the MDR (Bove et al., 1998; Aiyyer and Thorncroft, 2006). Over the last 5.0 ka, intense hurricane strikes in Puerto Rico are correlated with intervals of elevated El Niño-like events, as evidenced by precipitation activity in Ecuador (Moy et al., 2002; Donnelly and Woodruff, 2007). Similar comparisons can be made between El Niño-like events and hurricane strikes at TPBH (Fig. 7). Based on sedimentary and geochemical proxies, El Niño-like events decrease from ~1300 and 1400 AD (Moy et al., 2002; Conroy et al., 2008), which is within dating uncertainties for the onset of heightened activity at TPBH at 1350 AD. A longer-term period of reduced El Niño-like events follow until 1650 AD, whereafter evidence from Ecuador indicates that El Niño-like events again subtly increase (Moy et al., 2002). If one assumes that the modern relationship between El Niño years and tropical cyclogenesis operated over the last millennium, then the reduced El Niño activity from ~1350 to 1650 AD likely decreased vertical wind shear in the MDR, thus increasing the annual probability of cyclogenesis and contributing to the active interval detected in the northern Bahamas.

## 5.3. Comparison of TPBH to other Atlantic hurricane reconstructions

At this stage it is still early to complete a large-scale analysis of the changing frequency and intensity of Atlantic hurricane activity in the different sub-basins of the tropical Atlantic (e.g., Caribbean versus Gulf of Mexico versus North Atlantic). Such an analysis can only be accomplished with more observations of long-term hurricane activity throughout the entire Atlantic region. Given the available proxy records, however, the hurricane reconstruction from TPBH does share several similarities with other Atlantic

hurricane records, but it appears noticeably different from Gulf of Mexico hurricane reconstructions.

Over the last millennium, the AD 1400s appears to be a particularly active interval of Atlantic hurricane activity (Fig. 8). The mid-1400s experienced the most heightened hurricane activity in the Atlantic basin over the last millennium (Mann et al., 2009). In the northeast, Boldt et al. (2010) documented 7 overwash deposits during this period in cores taken from Mattaposisett Marsh, Massachusetts. This interval also encapsulates an intense hurricane strike on Whale Beach, New Jersey, between 1278 and 1438 AD (Donnelly et al., 2001a), multiple hurricane overwash deposits at Succotash Marsh (Donnelly et al., 2001b), and an intense hurricane strike in Vieques, Puerto Rico ~1475 AD (Donnelly and Woodruff, 2007). The Little Bahama Bank at TPBH also experienced heightened hurricane activity in the 1400s.

The record from TPBH also highlights differences in the hurricane activity between the northwestern Caribbean versus Gulf of Mexico. Lane et al. (2011) document increased hurricane activity in the northeastern Gulf of Mexico at Mullet Pond from 1200 to 1400 AD, which was an apparent quiescent interval at TPBH. It is important to note that both of these sites reside at very similar latitudes (Fig. 8). Although TPBH was hit by an event in the late 1200s, Mullet Pond was experiencing the most heightened hurricane activity of the last millennia during the 1200s. Conversely, the 1400s at Mullet Pond began a long-term reduction in intense hurricane events in the Gulf of Mexico, whereas activity at TPBH and throughout the Atlantic was elevated. In fact, it seems that precisely as hurricane activity at Mullet Pond is decreasing around 1350 AD, more storms are hitting TPBH (Fig. 8). A prominent hypothesis regarding paleo hurricane activity in the North Atlantic basin is that either the North Atlantic Oscillation (NAO) or the Intertropical Convergence Zone (ITCZ) is modulating hurricane migration pathways over the last 5.0 ka. This has been referred to as the Atlantic Hurricane Belt, the latitude of which is modulated by either the NAO or ITCZ (Liu and Fearn, 2000; Scott et al., 2003; McCloskey and Keller, 2009). Based on a k-means cluster analysis of Atlantic hurricane events from 1944 to 2000 AD (Elsner, 2003), the hurricane activity at TPBH (26° N) and Mullet Pond (29° N) over the last century should be similar given that they reside at very similar latitudes. But, evidence from TPBH suggests that this is not the case (Fig. 8). This anti-phasing of intense hurricane activity at similar latitudes between the North Atlantic and Gulf of Mexico seems to preclude a simple cause- and effect-relationship between the latitude of hurricane landfalls and a simple climate driver, and perhaps illustrates the complex regional differences between paleo hurricane activity.

An alternative hypothesis is that regional hurricane activity is not only related to climate variables encouraging intense hurricane cyclogenesis in the MDR (e.g., El Niño, West African Monsoon) or hurricane migration routes (e.g., NAO, ITCZ). Perhaps regional hurricane activity is also influenced by regional ocean-atmospheric conditions in the sub-basins of the North Atlantic Ocean, thus contributing to the spatial variability in Atlantic paleo hurricane records. Recently it was hypothesized that penetration of the Loop Current into the Gulf of Mexico may be an important variable impacting hurricane activity in the Gulf of Mexico versus the North Atlantic seaboard (Lane and Donnelly, 2012). Furthermore, SSTs in the Gulf of Mexico can vary independently from the MDR (Richey et al., 2007), and the Madden–Julian Index can further amplify cyclogenesis outside the MDR (Maloney and Hartmann, 2002). Both of these regional factors have the potential to either amplify or depress hurricanes originating in the MDR, or alternatively, encourage or discourage additional cyclogenesis. The regional variability in the ocean–climate system of different Atlantic sub-basins needs to be considered in an analysis of
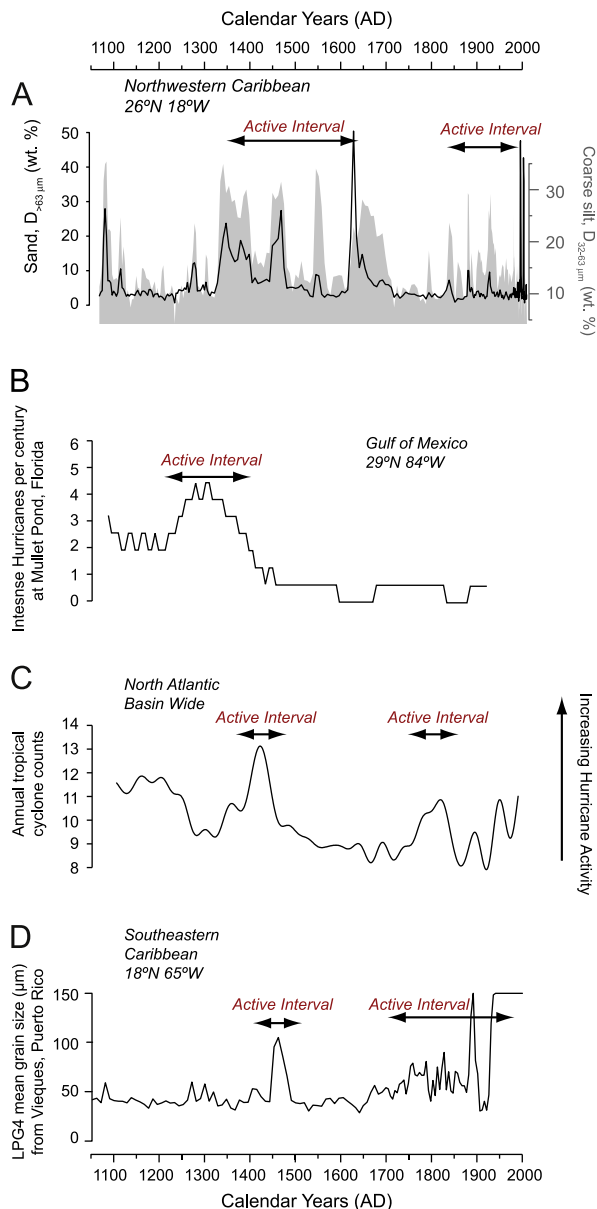
Fig. 8. Regional variability in hurricane activity between different sub-basins of the North Atlantic Ocean is highlighted by comparing the reconstruction of hurricane activity at TPBH (A) to reconstructions from the Gulf of Mexico (B, Lane et al., 2011), a basin-wide compilation (C, Mann et al., 2009), and the southeastern Caribbean region (D, Donnelly and Woodruff, 2007). Note that increasing hurricane activity in all panels is oriented upwards, and vertical scale is truncated scale in panel D.

Atlantic wide hurricane activity. Such analysis remains beyond the scope of this paper, which will require a wider observation network of paleo hurricane activity throughout the tropical Atlantic.

6. Conclusions

Previous research indicates that blueholes and sinkholes can archive hurricane induced overwash deposits, perhaps making these basins well suited to increasing our spatial network of paleo hurricane observations. As such, this study had two objectives: first, to evaluate bluehole sedimentation and the suitability of their successions to paleo hurricane research, and second, to generate a sorely needed reconstruction of prehistoric hurricane

activity in the northwestern Caribbean region. Overall, fine-grained carbonate mud is the dominant sediment being deposited into Thatchpoint Bluehole (TPBH) on the Little Bahama Bank. The high volume of fine carbonate mud dominated the standard grain size parameters (e.g., mean), and masked the signal of the coarse grained sedimentation. In contrast, the coarse grained sediments (coarse silts and sands) were highly sensitive to hurricane activity. After evaluating the sensitivity of TPBH to hurricane-induced sedimentation during the historic period, classic sand overwash deposits were produced during intense hurricane events (≥ category 3) striking within 50 km of TPBH in the historic period (Fig. 6A); and coarse silt deposition was related to either weak local hurricanes or intense hurricanes passing farther than 50 km away from TPBH. These results illustrate the varying effect of hurricane intensity on bluehole sedimentation, and may open new avenues of inquiry on how hurricane intensity has varied through time. Most importantly, these results support evidence that blueholes and sinkholes do contain valuable archives of paleo hurricane activity (Gischler et al., 2008; Lane et al., 2011).

Overall hurricane activity at TPBH, including all intensities of events, has been variable over the last millennium and linked to previously known hurricane climate forcings. A noteworthy quiescent interval occurs from 1150 AD to 1300 AD, coincident with increased El Niño activity and a weakened African Easterly Jet. Based on SSTs, the African Easterly Jet, and ENSO activity alone, the climate system at 1350 AD appears to begin creating favorable conditions for hurricane activity in the North Atlantic. By 1500 AD, hurricane activity was encouraged by elevated SSTs, invigorated West African Monsoon, and decreased El Niño events. After 1600 AD, the climate system was likely beginning to hamper cyclogenesis by decreasing SSTs and the African Easterly Jet, although depressed El Niño activity also persisted. Based on these relationships, one could hypothesize that perhaps the average intensity of hurricane events in the North Atlantic also peaked at 1500 AD, but testing this hypothesis will require additional hurricane reconstructions from other basins that are also calibrated to known hurricane intensities.

It appears that there is an anti-phase relationship between hurricane activity in the Gulf of Mexico versus the Atlantic regions through time after comparing the results from Thatchpoint Bluehole to previously available hurricane reconstructions. The exact climatological forcing behind these regional differences will only be understood with a larger database of paleo hurricane activity distributed throughout the tropical Atlantic, for which sinkholes and blueholes appear well poised to supply detailed reconstructions. Proxy-based hurricane reconstructions in the tropical Atlantic region are often interpreted as related to either (a) El Niño and West African Climate, or (b) migration of an Atlantic Hurricane Belt. However, hurricane activity at TPBH (northwest Caribbean, 26°N) and Mullet Pond (Gulf of Mexico, 29°N) appear anti-phased over the last millennium, yet these sites reside at similar latitudes. Perhaps regional ocean-atmospheric dynamics in different North Atlantic Ocean sub-basins may be playing a larger role modulating regional paleo hurricane activity than previously considered.

Appendix A. Supplementary material

Supplementary data associated with this article can be found in the online version at http://dx.doi.org/10.1016/j.csr.2013.04.032.

References

Aiyyer, A.R., Thorncroft, C., 2006. Climatology of vertical wind shear over the tropical Atlantic. Journal of Climate 19, 2969–2983.

Bell, G.D., Chelliah, M., 2006. Leading tropical modes associated with interannual and multidecadal fluctuations in North Atlantic Hurricane Activity. Journal of Climate 19, 590–612.

Black, D.E., Abahazi, M.A., Thunell, R.C., Kaplan, A., Tappa, E.J., Peterson, L.C., 2007. An 8-century tropical Atlantic SST record from the Cariaco Basin: baseline variability, twentieth-century warming, and Atlantic hurricane frequency. Paleoceanography 22 (PA4204), 10.

Blumenstock, D.I., 1958. Typhoon effects at Jaluit Atoll in the Marshall Islands. Nature 182 (4645), 1267–1269.

Blumenstock, D.I., Forsberg, F.R., Johnson, C.G., 1961. The re-survey of typhoon effects on Jaluit Atoll in the Marshall Islands. Nature 189 (4765), 618–620.

Boldt, K.V., Lane, P., Woodruff, J.D., Donnelly, J.P., 2010. Calibrating a sedimentary record of overwash from Southeastern New England using modeled historic hurricane surges. Marine Geology 275, 127–139.

Bove, M.C., Elsner, J.B., Landsea, C.W., Niu, X.F., O'Brien, J.J., 1998. Effect of El Niño on US landfalling hurricanes, revisted. Bulletin of the American Meterorological Society 79, 2477–2582.

Carew, J.L., Mylroie, J.E., 1997. Geology of the Bahamas. In: Vacher, H.L., Quinn, T.M. (Eds.), Geology and Hydrogeology of Carbonate Islands. Elsevier, Amsterdam, pp. 91–139.

Chenoweth, M., 1998. The early 19th century climate of The Bahamas and a comparison with 20th century averages. Climate Change 40, 577–603.

Conroy, J.L., Overpeck, J.T., Cole, J.E., Shanahan, T.M., Steinitz-Kannan, M., 2008. Holocene changes in eastern tropical Pacific climate inferred from a Galapagos lake sediment record. Quaternary Science Reviews 27, 1166–1180.

Dailey, P.S., Zuba, G., Ljung, G., Dima, I.M., Guin, J., 2009. On the relationship between North Atlantic sea surface temperatures and U.S. hurricane landfall risk. Journal of Applied Meteorology and Climatology 48, 111–129.

Davis, R.A.J., Knowles, S.C., Bland, M.J., 1989. Role of hurricanes in the Holocene stratigraphy of estuaries: examples from the gulf coast of Florida. Journal of Sedimentary Petrology 59 (6), 1052–1061.

deMenocal, P., Ortiz, J., Guilderson, T., Sarnthein, M., 2000. Coherent high- and low-latitude climate variability during the Holocene Warm Period. Science 288, 2198–2202.

Donnelly, J.P., Roll, S., Wengren, M., Butler, J., Lederer, R., Webb, T.I., 2001a. Sedimentary evidence of intense hurricane strikes from New Jersey. Geology 29 (7), 615–618.

Donnelly, J.P., Smith Bryant, S., Butler, J., Dowling, J., Fan, L., Hausmann, N., Newby, P., Shuman, B., Stern, J., Westhover, K., Webb, T.I., 2001b. 700 yr sedimentary record of intense hurricane landfalls in southern New England. Geological Society of America Bulletin 113, 715–727.

Donnelly, J.P., Woodruff, J.D., 2007. Intense hurricane activity over the past 5000 years controlled by El Niño and the West African Monsoon. Nature 447, 465–468.

Elsner, J.B., 2003. Tracking hurricanes. American Meteorological Society 84, 353–356.

Elsner, J.B., Bossak, B.H., Niu, X., 2001. Secular changs to the ENSO-U.S. hurricane relationship. Geophysical Research Letters 28, 4123–4126.

Elsner, J.B., Kossin, J.P., Jagger, T.H., 2008. The increasing intensity of the strongest tropical cyclones. Nature 455, 92–95.

Emanuel, K., Sundararajan, R., Williams, J., 2008. Hurricanes and global warming. American Meteorological Society 89, 347–367.

Emery, K.O., 1969. A Coastal Pond Studied by Oceanographic Methods. American Elsevier Publishing, New York.

Fairbanks, R.G., 1989. A 17,000-year glacio-eustatic sea level record: influence of glacial melting rates on the Younger Dryas even and deep-ocean circulation. Nature 342, 637–642.

García-Herrera, R., Gimeno, L., Ribera, P., Hernández, E., 2005. New records of Atlantic hurricanes from Spanish documentary sources. Journal of Geophysical Research 110 (D03109). (7 pp.).

Gischler, E., Shinn, E.A., Oschmann, W., Fiebig, J., Buster, N.A., 2008. A 1500-year Holocene Caribbean climate archive from the Blue Hole, Lighthouse Reef, Belize. Journal of Coastal Resarch 24 (6), 1495–1505.

Gischler, E., Zingeler, D., 2002. The origin of carbonate mud in isolated carbonate platforms of Belize, Central America. International Journal of Earth Sciences 91, 1054–1070.

Goldberg, P., Landsea, C.W., Mestas-Nunex, A.M., Gray, W.M., 2001. The recent increase in Atlantic hurricane activity: causes and implications. Science 293, 474–479.

Goldenberg, S.B., Landsea, C.W., Mestas-Nunex, A.M., Gray, W.M., 2001. The recent increase in Atlantic hurricane activity: causes and implications. Science 293, 474–479.

Goldenberg, S.B., Shapiro, L.J., 1996. Physical mechanisms for the association of El Niño and West African rainfall with Atlantic major hurricane activity. Journal of Climate 9, 1169–1187.

Heiri, O., Lotter, A.F., Lemcke, G., 2001. Loss on ignition as a method for estimating organic and carbonate content in sediments: reproducibility and comparability of results. Journal of Paleolimnology 25, 101–110.

Hua, Q., Barbetti, M., 2004. Review of tropospheric Bomb 14C data for carbon cylce modeling and age calibration purposes. Radiocarbon 46 (3), 1273–1298.

Keigwin, L.D., 1996. The little ice age and medieval warm period in the Sargasso sea. Science 274 (5292), 1504–1508.

Knutson, T.R., McBride, J.L., Chan, J., Emmanuel, K., Holland, G., Landsea, C., Held, I., Kossin, J.P., Srivastava, A.K., Sugi, M., 2010. Tropical cyclone and climate changes. Nature Geoscience 3, 157–163.

Kobluk, D.R., Lysenko, M.A., 1986. Reef-dwelling molluscs in open framework cavities Bonaire, N.A., and their potential for preservation in a fossil reef. Bulletin of Marine Science 39 (3), 656–672.

Landsea, C.W., 1993. A climatology of intense (major) Atlantic hurricanes. Monthly Weather Review 121, 1703–1713.

Lane, P., Donnelly, J.P., 2012. Hurricanes and typhoons—will tropical cyclones become stronger and more frequent? Pages News 20 (1), 33.

Lane, P., Donnelly, J.P., Woodruff, J.D., Hawkes, A.D., 2011. A decadally-resolved paleohurricane record archived in the late Holocene sediments of a Florida sinkhole. Marine Geology 287, 14–30.

Liu, K., Fearn, M.L., 2000. Reconstruction of prehistoric landfall frequencies of catastrophic hurricanes in NW Florida from lake sediment records. Quaternary Research 52 (2), 238–245.

Liu, K.-B., Fearn, M.L., 1993. Lake-sediment record of late Holocene hurricane activities from coastal Alabama. Geology 21 (9), 793–796.

Logan, A., Mathers, S.M., Thomas, M.L.H., 1984. Sessile invertebrate coelobite communities from reefs of Bermuda: species composition and distribution. Coral Reefs 2, 205–213.

Malaize, B., Bertran, P., Carbonel, P., Bonnissent, D., Charlier, K., Galop, D., Limbert, D., Serrand, N., Stouvenot, C., Pujol, C., 2011. Hurricanes in the Caribbean during the past 3700 years BP. The Holocene 21 (6), 911–924.

Maloney, E.D., Hartmann, D.L., 2002. Modulation of hurricane activity in the Gulf of Mexico by the Madden–Julian oscillation. Science 287, 2002–2004.

Mann, M.E., Woodruff, J.D., Donnelly, J.P., Zhang, Z., 2009. Atlantic hurricanes and climate over the past 1500 years. Nature 460, 880–885.

McCloskey, T.A., Keller, G., 2009. 5000 year sedimentary record of hurricane strikes on the central coast of Belize. Quaternary International 195, 53–68.

McIntyre, C.P., Roberts, M.L., Burton, J.R., McNichol, A.P., Burke, A., Robinson, L.F., von Reden, K.F., Jenkins, W.J., 2011. Rapid radiocarbon (^{14}C) analysis of coral and carbonate samples using a continuous-flow accelerator mass spectrometry system. Paleoceanography 26 (PA4212), 6.

McKee, E.D., 1959. Storm sediments on a Pacific Atoll. Journal of Sedimentary Petrology 29 (3), 354–364.

Michaels, P.J., Knappernberger, P.C., Davis, R.E., 2006. Sea-surface temperatures ad tropical cyclones in the Atlantic basin. Geophysical Research Letters 33 (L09708), 4.

Moy, C.M., Seltzer, G.O., Rodbell, D.T., Anderson, D.M., 2002. Variability of El Niño/ Southern Oscillation activity at millennial timescales during the Holocene. Nature 420, 162–165.

Mylroie, J.E., Carew, J.L., Moore, A.I., 1995a. Blue holes: definitions and genesis. Carbonates and Evaporites 10 (2), 225–233.

Mylroie, J.E., Carew, J.L., Vacher, H.L., 1995b. Karst development in the Bahamas and Bermuda. In: Curran, H.A. White, B. (Eds.), Terrestrial and Shallow Marine Geology of the Bahamas and Bermuda. Geological Society of America Special Paper 300, pp. 251–267.

Nguetsop, V.F., Servant-Vildary, S., Servant, M., 2004. Late Holocene climate changes in west Africa, a high resolution diatom record from equatorial Cameroon. Quaternary Science Reviews 23, 591–609.

Park, L.E., 2012. Comparing two long-term hurricane frequency and intensity records from San Salvador Island, Bahamas. Journal of Coastal Research 28, 891–902.

Pennington, W., Cambray, R.S., Fisher, E.M., 1973. Observations on lake sediments using fallout 137Cs as a tracer. Nature 242, 324–326.

Reading, A.J., 1990. Caribbean tropical storm activity over the past four centuries. International Journal of Climatology 10 (4), 365–376.

Reimer, P.J., Baillie, M.G.L., Bard, E., Bayliss, A., Beck, J.W., Blackwell, P.G., Ramsey, C. B., Buck, C.E., Burr, G.S., Edwards, R.L., Freidrich, M., Groots, P.M., Guilderson, T. P., Hajdas, I., Heaton, T.J., Hogg, A.G., Hughen, K.A., Kaiser, K.F., Kromer, B., McCormac, F.G., Manning, S.W., Reimer, R.W., Richards, D.A., Southon, J.R., Talamo, S., Turney, C.S.M., van der Plicht, J., Weyhenmeyer, C.E., 2009. IntCal09 and Marine09 radiocarbon age calibration curves, 0–50,000 years Cal BP. Radiocarbon 51 (4), 1111–1150.

Reimer, P.J., Brown, T.A., Reimer, R.W., 2004. Discussion: reporting and calibration of post-bomb 14C data. Radiocarbon 46 (3), 1299–1304.

Richey, J.N., Poore, R.Z., Flower, B.P., Quinn, T.M., 2007. 1400 yr multiproxy record of climate varibility from the northern Gulf of Mexico. Geology 35, 423–426.

Robbins, J.A., Edgington, D.N., 1975. Determination of recent sedimentation rates in Lake Michigan using Pb-210 and Cs-137. Geochimica Cosmochimica Acta 39, 285–304.

Roberts, M.L., von Reden, K.F., Burton, J.R., McIntyre, C.P. Beaupré, S.R. A gas-accepting ion source for Accelerator Mass Spectrometry: progress and applications. Nuclear Instruments and Methods in Physics Research B 294, 2013, 296–299.

Saenger, C., Cohen, A.L., Oppo, D.W., Halley, R.B., Carilli, J.E., 2009. Surface-temperature trends and variability in the low-lattitude North Atlantic since 1552. Nature Geoscience 2, 492–495.

Schwabe, S., Herbert, R.A., 2004. Black holes of the Bahamas: what they are and why they are black. Quaternary International 121, 3–11.

Scott, D.B., Collins, E.C., Gayes, P.T., Wright, E., 2003. Records of prehistoric hurricanes on the South Carolina coast based on micropaleontological and sedimentological evidence, with comparison to other Atlantic Coast records. Geological Society of America Bulletin 115 (9), 1027–1039.

Shanahan, T.M., Overpeck, J.T., Anchukaitis, K.J., Beck, J.W., Cole, J.E., Dettman, D.L., Peck, J.A., Scholz, C.A., King, J.W., 2009. Atlantic forcing of persistent drought in West Africa. Science 324, 377–380.

Shapiro, L.J., Goldenberg, S.B., 1998. Atlantic sea surface temperatures and tropical cyclone formation. Journal of Climate 11, 578–590.

Smart, P.L., Beddows, P.A., Doerr, S., Smith, S.L., Whitaker, F.F., 2006. Cave development on the Caribbean coast of the Yucatan Peninsula, Quintana Roo, Mexico. In: Harmon, R.S. Wicks, C. (Eds.), Perspectives on karst geomorphology, hydrology, and geochemistry—a tribute volume to Derek C. Ford and William B. White. Geological Society of America Special Paper 404, pp. 105–128.

Smart, P.L., Dawans, J.M., Whitaker, F., 1988. Carbonate dissolution in a modern mixing zone. Nature 355, 811–813.

Steadman, D.W., Franz, R., Morgan, G.S., Albury, N.A., Kakuk, B., Broad, K., Franz, S.E., Tinker, K., Pateman, M.P., Lott, T.A., Jarzen, D.M., Dilcher, D.L., 2007. Exceptionally well preserved late Quaternary plant and vertebrate fossils from a blue hole on Abaco, The Bahamas. In: Proceedings of the National Academy of Sciences 104 (50), 19897–19902.

van Hengstum, P.J., Scott, D.B., Gröcke, D.R., Charette, M.A., 2011. Sea level controls sedimentation and environments in coastal caves and sinkholes. Marine Geology 286, 35–50.

Webster, P.J., Holland, G.J., Curry, J.A., Chang, H.-R., 2005. Changes in tropical cyclone number, duration, and intensity in a warming environment. Science 1844, 1844–1846.

Woodruff, J.D., Donnelly, J.P., Emanuel, K., Lane, P., 2008. Assessing sedimentary records of paleohurricane activity using modeled hurricane climatology. Geochemistry Geophysics Geosystems 9 (Q09V10), 12.